J. Iron Steel Res. Int. (2020) 27:148–159
https://doi.org/10.1007/s42243-019-00296-w

ORIGINAL PAPER

Effect of direct charging of hot recycled slag on hot metal pretreatment dephosphorization in a dephosphorization furnace

Xue-feng Bai[1] · Yan-hui Sun[1] · Lei Luo[2] · Chang-liang Zhao[2]

Received: 26 November 2018 / Revised: 4 March 2019 / Accepted: 20 March 2019 / Published online: 17 July 2019

Abstract
Industrial experiments were carried out to investigate the effect of the direct charging of hot recycled slag (DCHRS) on hot metal pretreatment dephosphorization in a dephosphorization furnace. The bulk compositions of semi-steel and slag show that a better dephosphorization effect could be achieved by applying the DCHRS process in the dephosphorization furnace. Compared with the bulk compositions in normal heats, the mean contents of phosphorus in the semi-steel and total Fe in the final slag were decreased by 0.006 and 1.93 wt.%, respectively, with an increase of approximately 6 °C in the semi-steel temperature. According to mineralogical observations, the dephosphorization slags in normal heats and test heats were similar in petrographic constituents, but the metal loss was markedly decreased in the DCHRS process. Thermodynamic calculations show that even though the dephosphorization slag in the DCHRS process had the same dephosphorization capacity as that in the normal refining process, the phosphorus distribution between slag and hot metal in the new process was slightly higher and closer to the reaction equilibrium. Meanwhile, proper operating conditions, including slag basicity, total Fe content in the final slag, bath temperature, slag formation and slag volume, were optimized to improve the dephosphorization efficiency under the condition of the DCHRS process. The consumption of lime, light-burnt dolomite and oxygen during blowing was significantly decreased by the DCHRS process.

Keywords Dephosphorization · Hot slag · Slag recycling · Dephosphorization furnace · Thermodynamics

1 Introduction

Phosphorus is considered as one of the hazardous elements in steels. Excessive phosphorus dramatically increases the risk of brittle fracture at low temperature and degrades the impact toughness of steels [1, 2]. In addition, the defects in the local structure caused by the microsegregation of phosphorus during solidification can act as potential promoters of internal cracks in slabs [3, 4]. Hence, the removal of phosphorus is crucial during steel production [5]. Accordingly, various hot metal pretreatment dephosphorization processes including those using ladle, torpedo car and converter as the reaction vessels combined with various dephosphorizing agents have been adopted to meet the requirements for low- and ultra-low-phosphorus steel grades [6–16]. Compared with other reaction vessels, converters have a large freeboard with sufficient oxygen blowing capacity and excellent metal bath stirring by bottom gas blowing. Hence, the converter-type hot metal dephosphorization is more favorable to dephosphorization reactions in terms of thermal allowance and processing time [17, 18]. The converter-type dephosphorization has been developed into one of the most popular methods for hot metal pretreatment. On the other hand, the waste residue produced during the production of steel is usually reused in roads, cement production and other applications [19–21]. If the technique of slag recycling is directly applied in the refining process, refining costs and the influence of the technique on the environment can be primarily reduced by minimizing the total slag volume during refining [17, 22].

✉ Yan-hui Sun
sunyanhui@metall.ustb.edu.cn

[1] Collaborative Innovation Center of Steel Technology, University of Science and Technology Beijing, Beijing 100083, China

[2] Shougang Jingtang United Iron & Steel Co., Ltd., Tangshan 063200, Hebei, China

The recycling of converter slag as a dephosphorizing agent for converter-type hot metal dephosphorization has been a technique of utmost importance in the low-cost and high-efficiency production of clean steel [5, 23, 24]. As listed in Table 1, various recycling processes of basic oxygen furnace (BOF) slag during converter-type hot metal pretreatment can be classified into three general types according to the number of converters and the state of recycled slag. The multirefining converter (MURC) process is a typical slag recycling process [18, 25]. In the MURC process, the deslagging and slag-retaining operations were performed after dephosphorization and decarburization in the same converter, respectively. That is, the slag for the hot metal dephosphorization in the MURC process was actually the hot slag remaining after the decarburization in a previous heat. Therefore, both the total amount of exhausted slag and the heat loss during refining could be minimized by the reuse of hot recycled slag after decarburization. For the dephosphorization furnace (De-P furnace)–decarburization converter (De-C converter) duplex steelmaking process, the reutilization of the decarburization converter slag in the dephosphorization furnace is another typical converter slag recycling process. At Sumitomo Metal Industries, Ltd., a simple refining process (SRP) [26, 27] was adopted in the duplex steelmaking process. In this process, the decarburization converter slag containing less phosphorus oxide was recycled into the dephosphorization furnace. Hence, no decarburization converter slag was emitted from the process. Similar slag recycling techniques were introduced in other duplex steelmaking processes, such as the hot metal pretreatment furnace (H furnace)–BOF refining process (also called oxygen lime injection dephosphorization and desulfurization, OLIPS) [28], the LD (Linz–Donawitz) converter–optimized refining process (LD-ORP) [29, 30] and the Baosteel BOF refining process (BRP) [31]. Notably, the reused slag in a common duplex process was usually pretreated by the little water-spreading and heat-stewed methods and then charged into the dephosphorization furnace as the furnace burden by hopper [32]. Put it another way, unlike the MURC process, the recycled slag charged into the furnace in a traditional duplex process was in cold state. By contrast, Shougang Jingtang developed a process for direct charging of hot recycled slag (DCHRS) based on its own duplex steelmaking process. In the DCHRS process, the liquid-state hot recycled slag yielded from a decarburization converter (slag temperature of approximately 1500 °C) was directly charged into the dephosphorization furnace using a new slag vessel equipped with a redesigned division mouth. Thus, the DCHRS process provided efficient use of the heat of the hot recycled slag like the MURC process while retaining the advantage of duplex steelmaking processes [33].

Table 1 Various recycling processes of converter slag during hot metal pretreatment dephosphorization

Process	MURC	SRP	OLIPS	LD-ORP	BRP	DCHRS
Converter unit	1	2	2	2	2	2
Dephosphorization reactor	BOF	BOF	H furnace (slag method)	LD-ORP furnace	De-P furnace	De-P furnace
Heat size/t	8	250	80	290	300	300
Recycled slag state	Hot	Cold solid	Cold solid	Cold solid	Cold solid	Hot liquid
Flux	$CaO–CaF_2$–Fe ore	BOF slag–Fe ore–$CaO–CaF_2$	Flux top injection (CaO–mill scale–CaF_2), CaO–BOF slag–Mn ore	Flux bottom injection (CaO_3), $CaO–CaF_2$	$CaO–CaF_2$–BOF slag	BOF slag–cold-bonded pellets (–CaO–MgO)
Top gas blowing	O_2: 1000 (400, 1500) $m^3 h^{-1}$	O_2: 1.0–1.3 $m^3 t^{-1}$ min^{-1}	O_2: 100–120 $m^3 t^{-1}$ min^{-1}	O_2: 0.05–0.10 $m^3 t^{-1}$ min^{-1}	O_2: 0.83–1.67 $m^3 t^{-1}$ min^{-1}	O_2: 1.0 $m^3 t^{-1}$ min^{-1}
Bottom gas blowing	N_2: 200, 350 $m^3 h^{-1}$	CO_2: 0.05–0.20 $m^3 t^{-1}$ min^{-1}	–	N_2: 0. 05–0.10 $m^3 t^{-1}$ min^{-1}	N_2: 0.03–0.25 $m^3 t^{-1}$ min^{-1}	N_2: 0.17 $m^3 t^{-1}$ min^{-1}
Blowing time/min	–	8–10	–	~ 10	10–12	6–7
Source	Refs. [18, 25]	Refs. [27, 34]	Ref. [28]	Refs. [29, 30]	Ref. [31]	Current work

In the current study, the DCHRS process was tested in a dephosphorization furnace. Chemical and mineralogical analyses combined with thermodynamic calculations were performed to investigate the dephosphorization characteristics of the DCHRS process.

The specific objectives for this work are outlined as follows:

1. To examine the effects of the DCHRS process on dephosphorization reactions by investigating the composition changes of slag and hot metal in the dephosphorization furnace;
2. To elucidate the consumption of various raw materials and oxygen during dephosphorization;
3. To determine the mineralogical characteristics of slag during dephosphorization;
4. To analyze the dephosphorization capacity of slag based on thermodynamic investigations;
5. To establish the optimal conditions for dephosphorization during the DCHRS process.

2 Experimental procedure

2.1 Outline of DCHRS process

Industrial experiments were carried out using a 300 t dephosphorization furnace. The main production equipment in Shougang Jingtang contains two KR (Kambara reactors), two dephosphorization furnaces, three decarburization converters, two RH (Ruhrstahl–Heraeus) degassing vessels, two LF (ladle furnaces), two CAS (composition adjustment by sealed argon bubbling) and four continuous casters with two strands each. All hot metal must be desulfurized through the KR stirring process to ensure that the sulfur content was less than 0.002 wt.% before dephosphorization.

An overview of the DCHRS process between dephosphorization furnace and decarburization converter is depicted in Fig. 1. The dephosphorization slag in the DCHRS process mainly consists of the liquid-state hot recycled slag yielded from a decarburization converter. For the direct charging of the hot recycled slag, a 30 t slag vessel equipped with a division mouth was designed. After hot slag charging, cold-bonded pellets were added into the furnace to thicken the hot slag and furnace lining received effective protection by subsequent slag splashing, whereafter approximately 10 wt.% scrap was added into the furnace before hot metal charging. During blowing, the rates of the top-blown flow and bottom-blown flow were set at approximately 18,000 and 3000 $m^3\ h^{-1}$, respectively. Additionally, depending on the reaction state, small amounts of lime and light-burnt dolomite were charged into the furnace. The mean refining time per heat in the dephosphorization furnace was approximately 23 min.

Table 2 presents the data for the consumption of various raw materials and oxygen in test heats and normal heats. In normal heats, the slag-forming materials predominantly included lime, light-burnt dolomite and cold-bonded pellets. Thus, approximately 9.25 kg of lime and 3.66 kg of light-burnt dolomite per ton of hot metal were added into the furnace in the regular dephosphorization process. By

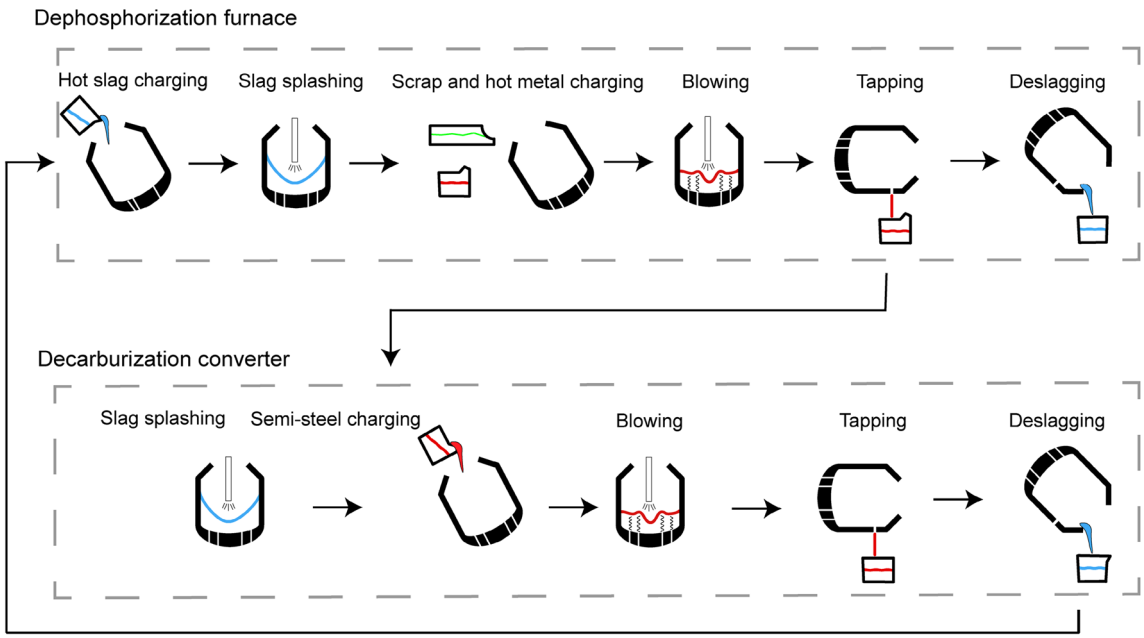

Fig. 1 Overview of DCHRS process

Table 2 Mean consumption of various raw materials and oxygen

Heat	Heat count	Raw material/(kg t^{-1})			Oxygen/(m^3 t^{-1})
		Lime	Light-burnt dolomite	Cold-bonded pellet	
Normal heat	91	9.25	3.66	14.17	9.67
Test heat	24	2.90	0.30	18.06	9.06

contrast, merely 2.90 kg of lime and 0.30 kg of light-burnt dolomite were consumed for each ton of hot metal when the new process was adopted. Furthermore, the heats with zero consumption of lime and dolomite accounted for approximately 42% and 46% of the total test heats, respectively. In contrast, the addition of cold-bonded pellets in the test heats was higher than that in normal heats for the rapid thickening of hot recycled slag. The point of this exercise is to promote the longevity of the lining through slight splashing and diminish the tendency of excessive splashing of hot metal and slag during the charging of hot metal. Additionally, the oxygen supplied for slag melting could be saved at the expense of the sensible heat of the premelted slag.

2.2 Experimental methods

The chemical compositions of the hot metal and slag samples collected in the present work were measured by optical emission spectrometry and X-ray fluorescence (XRF) spectrometry, respectively. Moreover, mineralogical analysis was performed to determine the physical and chemical characteristics of the slag, including its mineralogy, texture, constituents and distribution. Additionally, the relative amounts of minerals in the slag were examined using a metallographic microscope, which was described by the area fraction in the current work. For petrographic analysis, the slag sample was first broken and ground into fine particles smaller than 2 mm. These particles were then collected and inlayed into a petrographic specimen (10 mm in length and 15 mm in diameter) with epoxy glue. Then, the surface of the petrographic specimen was ground with SiC papers and subsequently polished with diamond paste. The mineralogical analysis was carried out using a metallographic microscope at magnification of 500–800. The total observed area of each specimen varied from 0.48 to 0.60 cm^2. The area percentage of phase i, X_i, was calculated as follows:

$$X_i = \frac{\sum_{j=1} x_j^i \cdot A_j}{\sum_{j=1} A_j} \times 100\% \quad (1)$$

where x_j^i is the area percentage of phase i in the field j and A_j is the area of field j.

3 Results and discussion

3.1 Evolution of composition of slag and hot metal in dephosphorization furnace

Table 3 shows the hot slag compositions of 24 heats from the decarburization converter, as determined using XRF analysis. The results in Table 3 show that the mean basicity of the hot slag reached 3.70 with the CaO content of 42.64 wt.%. Additionally, the TFe (total Fe) content was 19.74 wt.% on average, ranging from 16.90 to 24.07 wt.%. By contrast, the P_2O_5 content was only 1.65 wt.% on average and varied from 1.07 to 2.55 wt.%. Hence, the hot slag produced in the decarburization converter has a high potential for re-dephosphorization owing to its high basicity and low P_2O_5 content, which can simultaneously reduce the supply of lime in the dephosphorization furnace [22]. Moreover, the iron loss could be ameliorated to some extent through slag recycling, as suggested by the high TFe content in the decarburization converter slag.

To identify the effect of the DCHRS process on dephosphorization efficiency, hot metal samples collected from 24 test heats and 91 normal heats in the same time

Table 3 Composition of hot slag from decarburization converter

Item	CaO/wt.%	SiO_2/wt.%	MgO/wt.%	P_2O_5/wt.%	MnO/wt.%	FeO/wt.%	TFe/wt.%	Al_2O_3/wt.%	R
Maximum	46.70	14.07	10.22	2.55	2.95	30.95	24.07	5.29	4.44
Minimum	36.48	9.38	7.17	1.07	1.10	21.72	16.90	2.25	3.19
Average	42.64	11.62	8.71	1.65	1.72	25.38	19.74	3.08	3.70

$R = w(CaO)/w(SiO_2)$

frame were measured for the compositions of hot metal and semi-steel. The main results are shown in Table 4.

Table 4 shows that the difference in hot metal conditions between the two refining processes was not significant, whereas the mean value of the phosphorus content in semi-steel reached 0.0364 wt.% in test heats, approximately 0.006 wt.% lower than that in the normal heats. Simultaneously, the mean dephosphorization rate, η_P, in the test heats was 66.45%, showing an increase of 6.00% compared with that in the conventional process. These findings demonstrate the considerable advantage of the new process for dephosphorization reactions. Moreover, the average semi-steel temperature in the test heats rose by 6 °C to 1333 °C in the hot slag recycling trials due to the utilization of the sensible heat of the hot recycled slag.

The dephosphorization slag samples collected from 24 test heats and 91 normal heats over the same period were analyzed by XRF to obtain their chemical compositions. The results are listed in Table 5. The dephosphorization slags in various processes had approximately the same levels of CaO content and basicity with a decline of 1.93 wt.% in TFe content, indicating that the loss of metallic iron was reduced by the new process. In terms of oxygen balance in the decarburization process, the decrease in oxygen blowing combined with the increase in the oxidation reactions of [C] and [P] (Table 4) might lead to the reduction in TFe content in the test heats. In addition, according to the FeO prediction model by Su et al. [35] based on the oxygen balance mechanism and Levenberg–Marquardt neural network algorithm [36], the unfavorable dissolution of lime could lead to a rise in the FeO content. Considering the amount of lime and the heat returned from the hot slag, it seems that the FeO content in normal heats was more easily affected by the dissolution of lime. Thus, the difference of TFe content in the final dephosphorization slag between two processes may be further increased.

3.2 Petrographic constituents of slag during dephosphorization

Figure 2 shows the main petrographic results of the hot slag in the decarburization converter. In this work, the slag sample on hot metal was taken with iron rod. Since the samples were subjected to rapid cooling in water, it was

Table 4 Changes in composition and temperature of melt in dephosphorization furnace

Category	Stage	Heats count	Item	C/wt.%	Si/wt.%	Mn/wt.%	P/wt.%	S/wt.%	*T*/°C	η_P/%
Normal heats	Hot metal	91	Maximum	4.64	0.822	0.277	0.1350	0.00600	1399	
			Minimum	3.73	0.020	0.093	0.0735	0.00001	1297	
			Average	4.25	0.163	0.197	0.1068	0.00080	1344	
	Semi-steel	91	Maximum	3.62	0.085	0.227	0.0706	0.00900	1357	80.30
			Minimum	2.81	0.012	0.004	0.0217	0.00210	1282	26.88
			Average	3.26	0.021	0.040	0.0420	0.00500	1327	60.45
Test heats	Hot metal	24	Maximum	4.45	0.310	0.236	0.1250	0.00200	1384	
			Minimum	3.67	0.039	0.095	0.0840	0.00001	1312	
			Average	4.29	0.158	0.201	0.1085	0.00060	1345	
	Semi-steel	24	Maximum	3.89	0.067	0.140	0.0700	0.00700	1409	88.80
			Minimum	2.95	0.012	0.007	0.0110	0.00500	1291	28.12
			Average	3.24	0.026	0.053	0.0364	0.00500	1333	66.45

T Melting temperature

Table 5 Slag composition in dephosphorization furnace

Category	Item	CaO/wt.%	SiO_2/wt.%	MgO/wt.%	P_2O_5/wt.%	MnO/wt.%	FeO/wt.%	TFe/wt.%	Al_2O_3/wt.%	*R*
Normal heat	Maximum	38.01	22.09	7.41	10.74	15.81	45.90	35.70	4.99	2.80
	Minimum	19.69	12.69	4.30	2.20	4.07	7.98	6.21	1.42	1.10
	Average	30.70	15.69	5.38	6.53	10.26	14.68	11.29	2.53	1.97
Test heat	Maximum	42.87	20.90	7.26	8.85	12.43	34.92	27.17	6.40	2.45
	Minimum	22.80	13.34	4.96	2.47	5.30	7.93	6.17	1.74	1.15
	Average	31.81	16.18	5.91	5.87	8.69	12.17	9.36	2.92	2.00

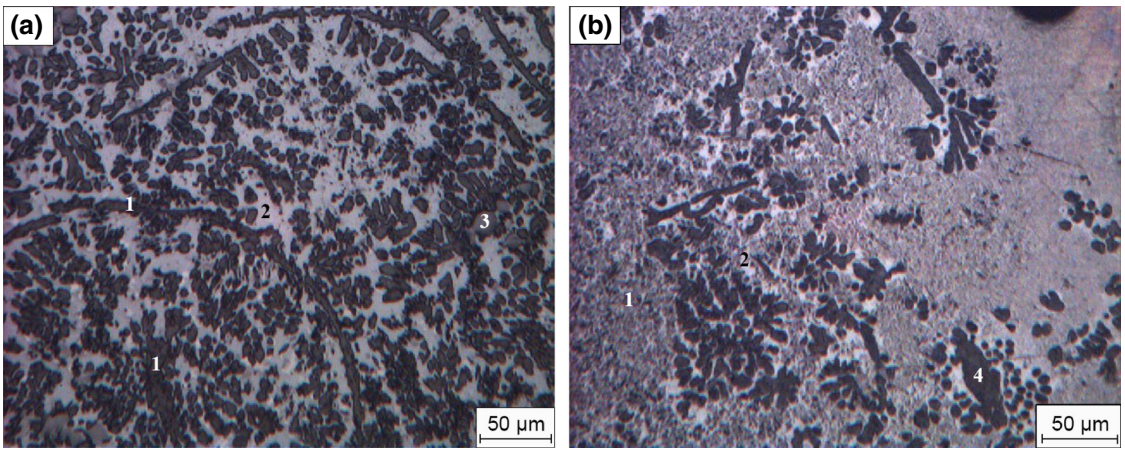

Main phase	1—C_2S	2—RO	3—(Mg, Fe)O	4—C_3S
Area percentage/%	60–65	25–30	5–7	1–3

Fig. 2 Petrographic analysis of hot recycled slag

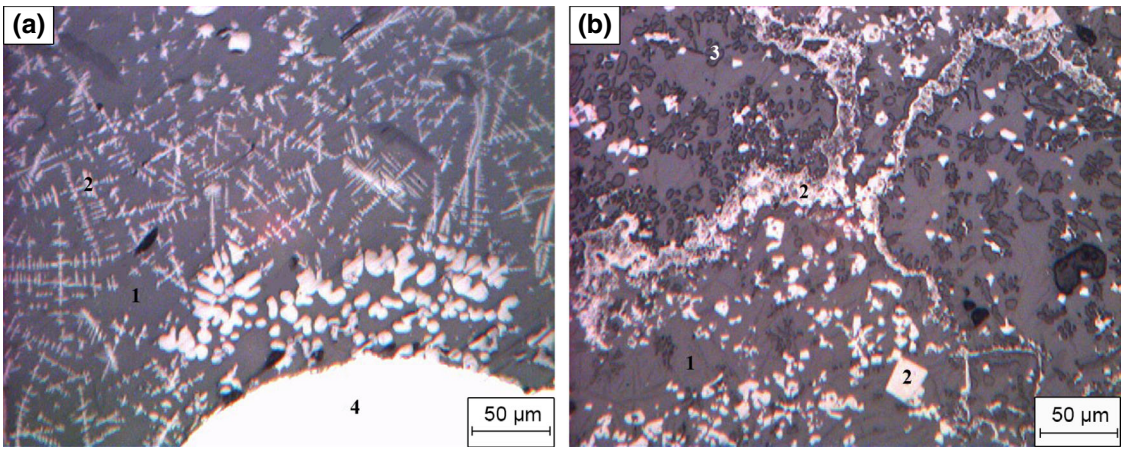

Phase	1—Glass phase	2—Wustite	3—C_2S	4—Metallic iron
Area percentage/%	50–55	15–20	5–10	15

Fig. 3 Petrographic analysis of final dephosphorization slag in normal process

believed that the mineralogical phase of samples should be maintained without significant transformation during the solidification. As shown in Fig. 2, Ca_2SiO_4 (C_2S) was the dominant mineral phase accounting for 60%–65% of the viewing area and presented a granular shape by cross-sectional investigations. That is, the abundance of C_2S phase in the hot slag provided the main function of replacing CaO in lime for the second dephosphorization in the DCHRS process. As the second most abundant phase, the RO phase, which is a solid-state solution composed mainly of FeO, MnO, MgO and CaO, comprised approximately 25%–30% of the total field of view. In addition, a minor amount of granule-shaped ferropericlase phase ((Mg, Fe)O) as well as lath-like Ca_3SiO_5 phase (C_3S) could be observed through the metallographic microscope as shown in Fig. 2.

Figure 3 presents the results of mineralogical analysis of the slag at the endpoint of blowing in the normal process. The slag during the dephosphorization was generally considered as multiphase flux that comprised both solid and liquid [37–39]. As shown in Fig. 3, the petrographic constituent included glass phase, wustite, C_2S and metallic iron. The dark gray region with area percentage of 50%–55% corresponded to the glass phase. Approximately 10%–15% of the total area was wustite phase, of which cross section had the shapes of granule and dendrite. Meanwhile, the metallic iron phase was still observed under the

metallographic microscope, of which area percentage was approximately 15%.

Figure 4 shows the petrographic analysis of the final dephosphorization slag in the slag recycling process. Overall, the dephosphorization slag in test heats had similar petrographic constituents as that in normal heats. The glass phase, as a mineral substrate, represented 65%–70% of the viewing field. Furthermore, the surface of the slag petrographic phase was smooth and well developed, implying that the slag had better melting effects. Notably, several investigations have identified the considerable role of the solid phase C_2S in condensing P, while the phosphorus content in the liquid phase was relatively low [37, 38, 40]. Therefore, for the minimization of P concentration in semi-steel, the ability of the C_2S to condense P should be enhanced [18]. However, there seemed to be no significant disparity in C_2S content between two different processes according to the results of petrographic analysis. A possible explanation for this result may be the insignificant difference of phosphorus in semi-steel at ppm level. This, in turn, provides further evidence that the dephosphorization capacity of slag in the DCHRS process closely approximated that in the normal process in terms of C_2S content. In addition, compared with the petrographic results in Fig. 3, there were obvious decreases in the area fractions of both metallic iron and wustite, suggesting that the new process was conducive to improving the iron yield.

3.3 Thermodynamics for dephosphorization capacity of slag

The dephosphorization potential of the slag can be estimated based on its phosphate capacity, $C_{PO_4^{3-}}$, which can be calculated using Eq. (2) [41, 42]. The phosphate capacity in Eq. (2) is expressed as a function of temperature and slag composition on a mass percent basis, indicating that an appropriately low temperature in the bath and a proper slag composition are indispensable for the phosphorus collection in the slag. Figure 5 shows the phosphate capacity of the dephosphorization slag in various heats. As shown in Fig. 5, no considerable difference was observed in phosphate capacity between the two different refining processes. This finding indicates that in terms of the phosphate capacity of slag, the dephosphorization slag in the DCHRS process had the same dephosphorization potential as that in the conventional refining process.

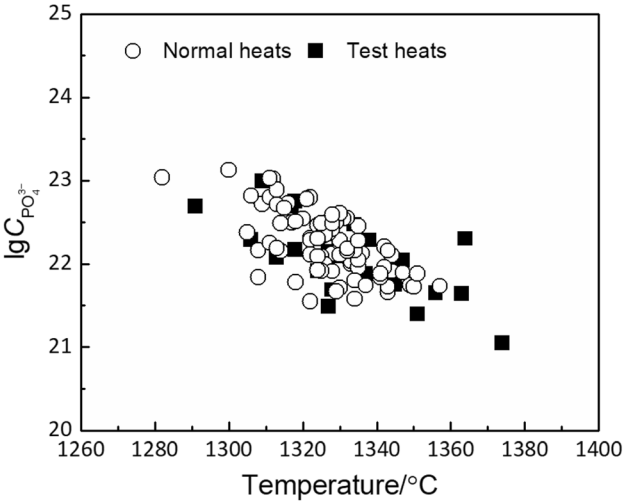

Fig. 5 Phosphate capacity of dephosphorization slag

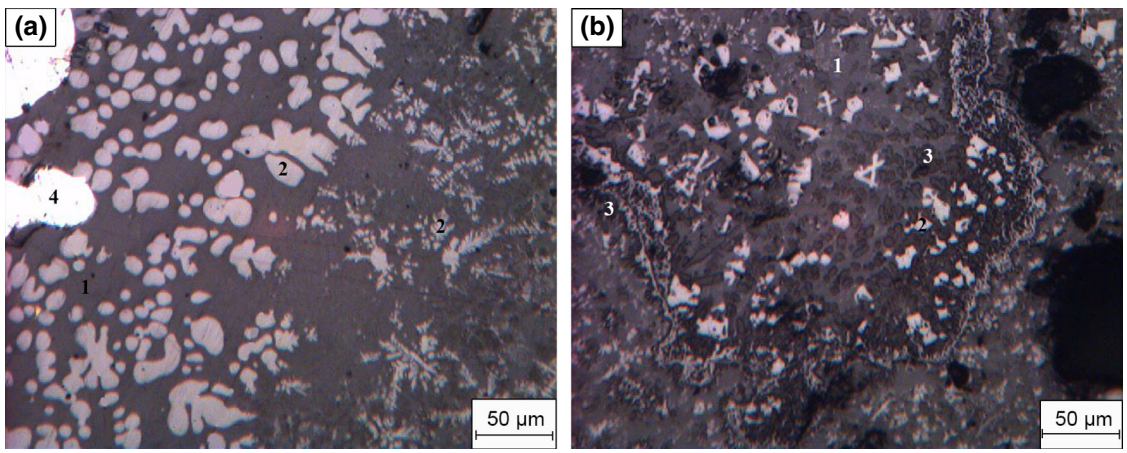

Phase	1—Glass phase	2—Wustite	3—C_2S	4—Metallic iron
Area percentage/%	65–70	10–15	5–10	5

Fig. 4 Petrographic analysis of final dephosphorization slag in DCHRS process

$$\lg C_{PO_4^{3-}} = 0.0938\{w(CaO) + 0.50w(MgO) + 0.30w(Fe_tO) + 0.35w(P_2O_5) + 0.46w(MnO)\} + 54,180/T - 15.87 \quad (2)$$

The phosphorus distribution between slag and hot metal is also an effective parameter for evaluating the dephosphorization state in the furnace using the semi-steel chemistry and temperature at the blow ends of dephosphorization. In the current work, the phosphorus distribution is defined as $L_P = w(P)/w[P]$, where L_P is the distribution of P between slag and hot metal, and $w(P)$ and $w[P]$ are the phosphorus mass fractions in the slag and the hot metal, respectively. The equilibrium P distribution was predicted using the Healy-type dephosphorization formula [43] modified by Suito and Inoue [41] as follows:

$$\lg \frac{w(P)}{w[P]w(TFe)^{5/2}} = 0.0720[w(CaO) + 0.3w(MgO) + 0.6w(P_2O_5) + 0.2w(MnO) + 1.2w(CaF_2) - 0.5w(Al_2O_3)] + 11,570/T - 10.52 \quad (3)$$

Considering the reduction of Fe_tO in slag by carbon, the value of L_P based on the slag–metal laboratory experiment cannot accurately reflect the practical equilibrium P distribution between Fe_tO-containing slag and hot metal. Therefore, in order to estimate the value of phosphorus distribution at the temperature of hot metal treatment L_P^h, the extrapolated L_P by Eq. (3) should be transformed into Eq. (4).

$$\lg L_P^h = \lg L_P + \frac{1873}{T}\left\{e_P^C w[C] + \gamma_P^C (w[C])^2\right\} \quad (4)$$

where $w[C]$ is the C concentration in metal and e_P^C and γ_P^C are the first-order and the second-order interaction parameters at 1873 K, which are considered to be 0.126 and 0.014 [44], respectively.

Thus, the calculated phosphorus distribution during hot metal treatment can be expressed by Eq. (5):

$$\lg L_P^h = 2.5\lg w(TFe) + 0.0720[w(CaO) + 0.3w(MgO) + 0.6w(P_2O_5) + 0.2w(MnO) + 1.2w(CaF_2) - 0.5w(Al_2O_3)] + 11,570/T - 10.52 + 1873\left\{e_P^C w[C] + \gamma_P^C (w[C])^2\right\}/T \quad (5)$$

The calculated and measured values of $\lg L_P^h$ for the conventional process and the DCHRS process are shown in Fig. 6. The measured value of L_P^h in the DCHRS process was slightly higher and was closer to the calculated value in the test heats, implying that the recycling of hot slag can promote the reaction equilibrium between slag and hot metal in the dephosphorization furnace.

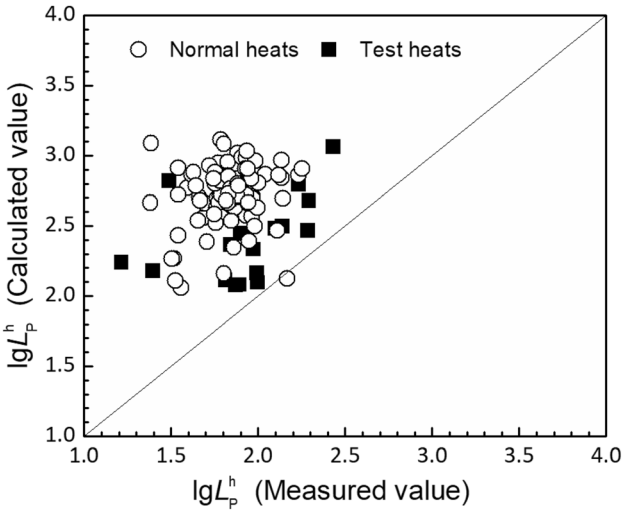

Fig. 6 Phosphorus distribution between slag and hot metal

3.4 Improvement in dephosphorization efficiency during DCHRS process

One of the most direct benefits of the reutilization of hot slag is to decrease or even entirely eliminate the addition of lime during blowing. However, the recycling process of hot slag can be applied in the dephosphorization furnace only if the dephosphorization efficiency is sufficiently high.

Figure 7 shows the influence of slag basicity on dephosphorization in the DCHRS process in a dephosphorization furnace. As shown in Fig. 7, the mean value of the phosphorus content in semi-steel decreased with increasing the slag basicity. The recommended value of slag basicity in the dephosphorization furnace was approximately 2.0, where a steady and high dephosphorization rate with a low phosphorus content in the semi-steel could be obtained. A higher dephosphorization efficiency could certainly be achieved by increasing the value of $w(CaO)/w(SiO_2)$ in the slag, as shown in Fig. 7, depending on the grade of the steel.

The relationship between TFe content and phosphorus distribution in a dephosphorization furnace for the DCHRS process can be estimated using Eq. (5). For the prediction, some compositions of the slag were fixed and taken as follows: MgO 6 wt.%, P_2O_5 6 wt.%, MnO 9 wt.% and Al_2O_3 3 wt.%. The FeO content in the slag was calculated using the TFe content. In the present work, the temperature and $w[C]$ in metal were assumed to be 1340 °C and 3.2, respectively. Thus, the modified Healy-type dephosphorization formula [41] at the temperature of hot metal treatment can be expressed using the fixed composition by Eq. (6):

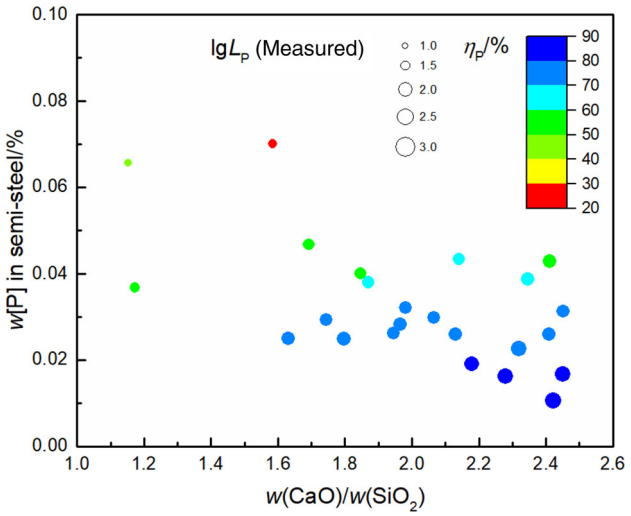

Fig. 7 Dependence of dephosphorization on slag basicity for DCHRS process in a dephosphorization furnace

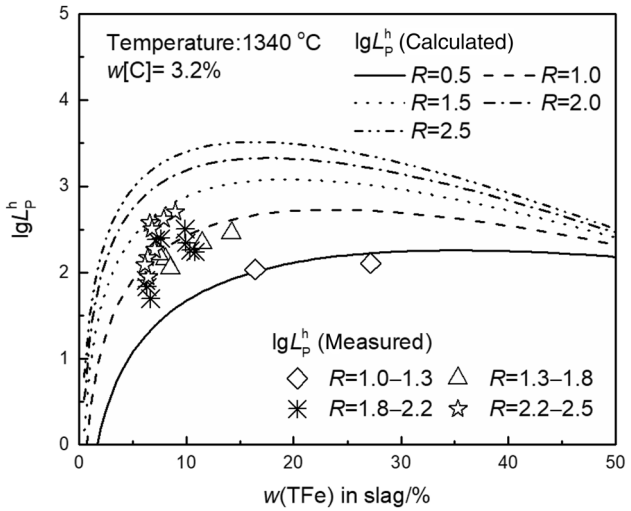

Fig. 8 Effect of TFe content on phosphorus distribution during DCHRS process

$$\lg\frac{w(\mathrm{P})}{w[\mathrm{P}]} = 2.5\lg w(\mathrm{TFe}) + \frac{0.0720w(\mathrm{CaO})/w(\mathrm{SiO_2})}{1+w(\mathrm{CaO})/w(\mathrm{SiO_2})}\times\left[76-\frac{M_{\mathrm{FeO}}}{M_{\mathrm{Fe}}}w(\mathrm{TFe})\right]-2.35 \tag{6}$$

where M_{FeO} and M_{Fe} denote the relative molecular mass and relative atomic mass of FeO and Fe, which are considered to be 71.85 and 55.85, respectively. The results are illustrated in Fig. 8.

Figure 8 shows that as the basicity increased from 1.0 to 2.0, the calculated $\lg L_{\mathrm{P}}^{\mathrm{h}}$ value increased from approximately 2.43 to 3.19 for the slag containing 10 wt.% TFe, revealing that a relatively higher basicity was also required for deep dephosphorization. In Fig. 8, the phosphorus distribution increased substantially with the increase in TFe content when the TFe content was controlled to be less than 10 wt.% at $w(\mathrm{CaO})/w(\mathrm{SiO_2}) = 2.0$. Therefore, the task of dephosphorization could also be fulfilled with an appropriately low TFe slag, consistent with the results of previous work [22, 25]. Nevertheless, as presented in Fig. 8, a too high TFe content cannot lead to the expected increase in phosphorus distribution due to dilution of slag basicity, which instead increased the metal loss. Consequently, the TFe concentration in the slag should be controlled to 10–15 wt.% at $w(\mathrm{CaO})/w(\mathrm{SiO_2}) = 2.0$.

A lower temperature can promote the phosphorus distribution between hot metal and the slag [22], which can be estimated using the modified Healy-type dephosphorization formula [41] as presented in Eq. (5). For the calculation, several components of the slag were fixed as follows: MgO 6 wt.%, P_2O_5 6 wt.%, MnO 9 wt.% and Al_2O_3 3 wt.%. The FeO content in the slag was calculated using the TFe content that was assumed to be 10 wt.%. The carbon content in metal was assumed to be 3.2 wt.%. Thus, the relation between the P distribution and bath temperature with various slag basicities can be expressed by Eq. (7):

$$\lg\frac{w(\mathrm{P})}{w[\mathrm{P}]} = \frac{4.5457w(\mathrm{CaO})/w(\mathrm{SiO_2})}{1+w(\mathrm{CaO})/w(\mathrm{SiO_2})} + 12,600/T - 7.61 \tag{7}$$

Figure 9 shows the effects of temperature at the blow ends of dephosphorization on the distribution of P with various slag basicities in the DCHRS process. As the temperature decreased from 1400 to 1300 °C, the calculated value of $\lg L_{\mathrm{P}}^{\mathrm{h}}$ increased from 2.95 to 3.43 at $R = 2.0$. Looking at Fig. 10, it is apparent that the state of dephosphorization in the furnace did not reach equilibrium

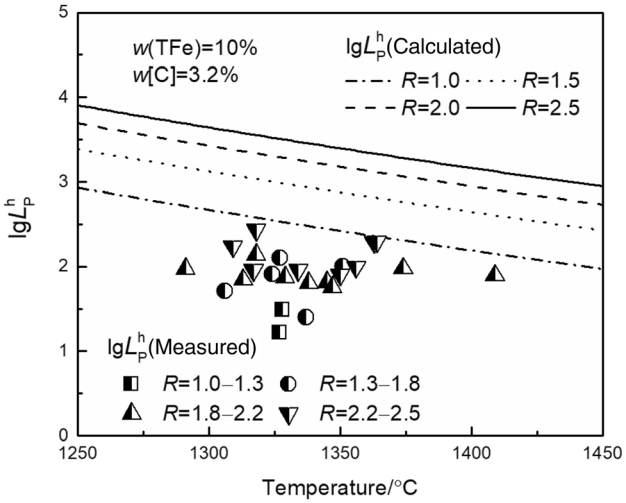

Fig. 9 Dependence of phosphorus distribution on temperature during DCHRS process

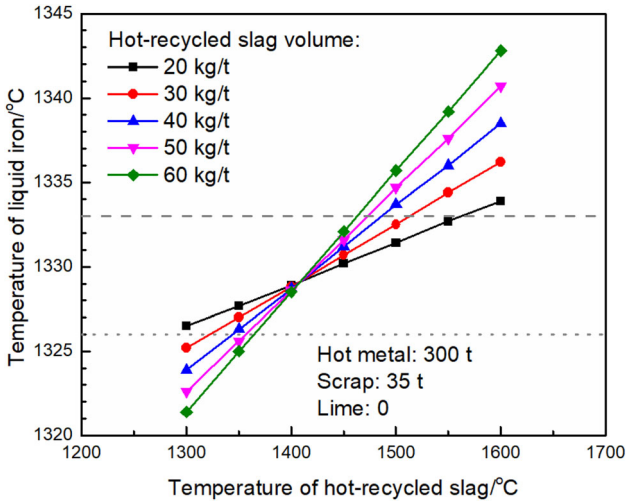

Fig. 10 Effect of hot recycled slag volume on heat balance in dephosphorization furnace

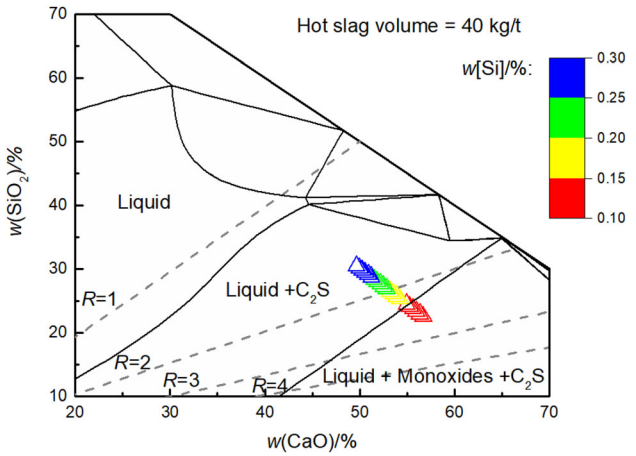

Fig. 11 Effect of initial Si content on slag formation in dephosphorization furnace

yet. However, an excessively low semi-steel temperature adversely affected the smooth operation, unexpectedly increasing the cost of the subsequent refining in the decarburization converter. Based on the calculated results and the operational conditions, the adequate temperature in the dephosphorization furnace during the DCHRS process was between 1300 and 1350 °C.

The nature for improving the efficiency of dephosphorization in the DCHRS process is to minimize heat loss and accelerate slag formation by the utilization of the sensible heat of the recycled slag. In order to separate the influence of the hot slag on the heat balance in the dephosphorization furnace, a heat balance model established by Zhao [45] was introduced into this work. For the calculation, the lime consumption was set at zero and 35 t of scrap in total was charged into the furnace (300 t). The predicted results are presented in Fig. 10. The dash line and dot line in Fig. 10 represent the mean temperatures of hot metal and semi-steel in normal heats, respectively. At the hot slag temperature of 1500 °C, as the slag volume increased from 20 to 60 kg t^{-1}, there was approximately an increase of 4 °C in the temperature of semi-steel. Moreover, the effect of the slag volume on the heat balance was significantly enhanced by increasing the returned slag temperature according to the predicted results. Thus, compared with the dissolution of lime, a rapid slag formation and a good melting effect could be accomplished during the DCHRS process, thereby promoting the dephosphorization reactions at the interface between hot metal and slag. The current calculations are consistent with the results from petrographic analysis.

Figure 11 shows the calculated slag formation with various initial Si contents in the hot metal when 40 kg t^{-1} of the reused slag (close to the output per heat in decarburization slag) was added into the furnace. The positive triangles in the figure represent the slag compositions at various initial Si contents ranging from 0.1 to 0.3 wt.% at intervals of 0.1 wt.%. Meanwhile, the $CaO–SiO_2–FeO$ phase diagram with Fe saturation at 1340 °C (calculated using FactSage 7.0 [46]) combined with the iso-basicity is also presented in Fig. 11. The prediction model was established based on the converter material balance reported by Zhao et al. [47]. The desilication rate in the current calculation was 86% for 0.10 wt.% ≤ w[Si] ≤ 0.15 wt.% and 92% for 0.15 wt.% ≤ w[Si] ≤ 0.30 wt.%, respectively. The pig iron mass was 300 t per heat with approximately 5.4 t of cold-bonded pellets. In Fig. 11, as the value of the Si content increased from 0.1 to 0.3 wt.%, the slag composition point in the $CaO–FeO–SiO_2–Fe_{sat.}$ phase diagram moved from "Liquid + Monoxide + C_2S" into the "Liquid + C_2S" region. Simultaneously, the basicity of the dephosphorization slag decreased from approximately 2.5 to 1.6. According to Fig. 7, the suitable basicity of dephosphorization slag should be controlled at approximately 2.0. Therefore, lime consumption was theoretically not required for slag formation when w[Si] = 0.19 wt.% with 40 kg recycled slag per ton of hot metal charged into the furnace. Otherwise, a moderate amount of lime was expected to be added into the furnace to adjust the slag basicity.

The effects of hot recycled slag volume on slag formation in the dephosphorization furnace during the DCHRS process are predicted in Fig. 12. The inverted triangles in Fig. 12 denote the slag compositions at various amounts of returned slag in the range from 0 to 120 kg t^{-1} at intervals of 0.1 kg t^{-1}, when the initial Si content in the hot metal is 0.15 wt.%. As presented in Fig. 7, the appropriate value of slag basicity for dephosphorization should be controlled at approximately 2.0. Therefore, for w[Si] = 0.15 wt.%, the theoretical amount of slag charged into the furnace was 6.93–11.50 kg t^{-1} as the slag basicity varied

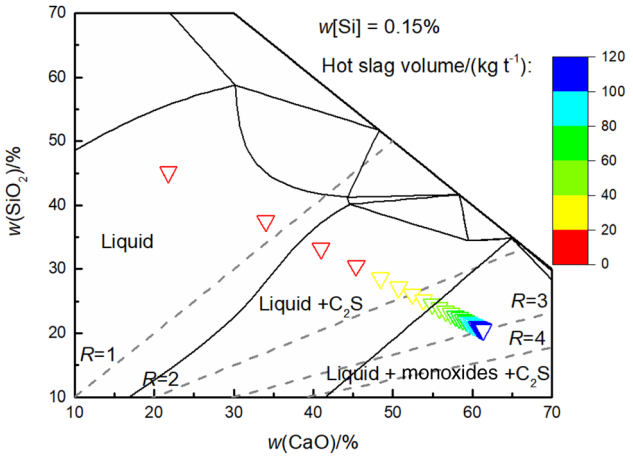

Fig. 12 Effect of hot slag volume on slag formation in dephosphorization furnace

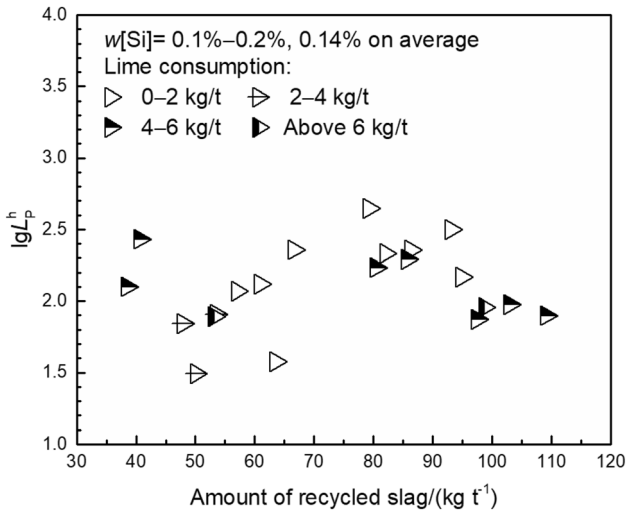

Fig. 13 Effect of slag volume on dephosphorization during DCHRS process

from 1.8 to 2.2. Notably, the calculated theoretical slag volume represents the minimum amount of hot slag for dephosphorization, implying that some operational factors such as lining protection by slight slag splashing were not included in the present estimation.

Figure 13 shows the practical consequences of the differences in hot slag volume on the phosphorus distribution with various values of lime addition in the dephosphorization furnace. As shown in Fig. 13, the values of the phosphorus distribution between slag and hot metal were increased with the addition of the returned slag. However, when the slag amount exceeded approximately 80 kg per ton of hot metal, the value of $\lg L_P^h$ showed no distinct increase, even though more lime was charged into the furnace. This result could be attributed to the limited mass transfer at the interface between hot metal and slag. Furthermore, on the basis of operational experience, the excessive charging of returned slag into the furnace gave rise to the splashing of hot metal and slag during the pouring of molten pig iron. Additionally, the slag generated in the decarburization converter was only 30–40 kg per ton of steel when the less slag steelmaking process was adopted in the decarburization converter. As a result, the smelting rhythm of the duplex process inevitably produced a considerable influence on the application of slag recycling process. Fortunately, as shown in Fig. 13, a satisfactory dephosphorization result can still be achieved by charging some lime into the furnace in the case of limited hot slag output.

4 Conclusions

1. A better dephosphorization effect was obtained during the DCHRS process in the dephosphorization furnace. After the DCHRS process was adopted, the endpoint phosphorus content in the semi-steel and the TFe content in the final slag were reduced on average by 0.006 and 1.93 wt.%, respectively, while an increase of approximately 6 °C in the semi-steel temperature was generated in the DCHRS process.
2. The consumption of lime, dolomite and oxygen was substantially decreased owing to the application of the DCHRS process in the dephosphorization furnace. However, more cold-bonded pellets were consumed in test heats for the rapid thickening of hot recycled slag.
3. The petrographic constituents of hot recycled slag and dephosphorization slags were obtained. The dephosphorization slags in different processes had similar petrographic constituents, but metal loss was significantly reduced in the DCHRS process.
4. According to thermodynamic calculations, there was no significant difference in the phosphate capacity of the dephosphorization slag between the two different slag formation processes. However, the distribution of phosphorus in test heats was slightly higher and closer to the equilibrium between hot metal and slag due to the recycling of the hot slag.
5. The DCHRS process was optimized for higher dephosphorization efficiency. The effects of slag basicity, TFe content and temperature on dephosphorization reactions in the DCHRS process were established. The appropriate amount of hot slag charged into the dephosphorization furnace depends on the Si content of the pig iron, the final slag basicity and the slag output of the decarburization converter.

Acknowledgements This work was financially supported by the National Natural Science Foundation of China (51574026).

References

[1] Res. Gp. of Phosphorus Segregation, Acta Metall. Sin. 17 (1981) 124–129.
[2] Z.H. Tian, L.Q. Ai, K.K. Cai, Steelmaking 19 (2003) No. 6, 13–18.
[3] J.H. Liu, Y.P. Bao, W. Sun, S.Q. Huang, J. Zhou, Iron and Steel 41 (2006) No. 8, 37–40.
[4] L.C. Xiu, J.C. Gao, Z.H. Zhao, Steelmaking 23 (2007) No. 4, 25–28.
[5] C.Z. Yang, G. Wei, J.H. Liu, J.T. Song, Steelmaking 28 (2012) No. 3, 1–6, 10.
[6] K. Sasaki, Y. Ohkita, T. Ikeda, T. Okazaki, T. Matsuo, A. Kawami, Tetsu-to-Hagane 63 (1977) 1801–1808.
[7] T. Ikeda, T. Matsuo, Trans. ISIJ 22 (1982) 495–503.
[8] K. Marukawa, S. Anezaki, I. Yamazaki, Tetsu-to-Hagane 69 (1983) 1856–1862.
[9] N. Masumitsu, K. Ito, R.J. Fruehan, Metall. Trans. B 19 (1988) 643–648.
[10] C. Nassaralla, R.J. Fruehan, D.J. Min, Metall. Trans. B 22 (1991) 33–38.
[11] G.Q. Li, T. Hamano, F. Tsukihashi, ISIJ Int. 45 (2005) 12–18.
[12] R. Inoue, H. Suito, ISIJ Int. 46 (2006) 188–194.
[13] S. Basu, A.K. Lahiri, S. Seetharaman, J. Halder, ISIJ Int. 47 (2007) 766–768.
[14] Y.C. Lü, X.H. Wang, G.S. Zhu, H.B. Li, Chinese Journal of Engineering 38 (2016) 335–341.
[15] W. Wu, S.F. Dai, Y. Liu, J. Iron Steel Res. Int. 24 (2017) 908–915.
[16] X.F. Bai, C. Zhuo, B. Huang, Z.C. Zhao, Y.H. Sun, X.T. Liang, L. Chen, J. Chen, Chinese Journal of Engineering 40 (2018) S1, 85–92.
[17] S.Y. Kitamura, K. Yonezawa, Y. Ogawa, N. Sasaki, Ironmak. Steelmak. 29 (2002) 121–124.
[18] N. Sasaki, Y. Ogawa, S. Mukawa, K.I. Miyamoto, Nippon Steel Tech. Rep. (2013) No. 104, 26–32.
[19] C.J. Shi, J.S. Qian, Resour. Conserv. Recycl. 29 (2000) 195–207.
[20] N. Ortiz, M.A.F. Pires, J.C. Bressiani, Waste Manage. (Oxford) 21 (2001) 631–635.
[21] P. Chaurand, J. Rose, V. Briois, L. Olivi, J.L. Hazemann, O. Proux, J. Domas, J.Y. Bottero, J. Hazard. Mater. 139 (2007) 537–542.
[22] K.D. Xu, L.J. Xiao, Y. Gan, L. Liu, X.H. Wang, Acta Metall. Sin. 48 (2012) 1–10.
[23] J.X. Li, X.D. Hao, S.T. Qiu, P. Zhao, J. Univ. Sci. Technol. Beijing 31 (2009) 970–973.
[24] T. Emi, ISIJ Int. 55 (2015) 36–66.
[25] Y. Ogawa, M. Yano, S. Kitamura, H. Hirata, Tetsu-to-Hagane 87 (2001) 21–28.
[26] K. Yoshida, Y. Tozaki, T. Matsuo, N. Aoki, Y. Yoshiyama, Steel Times Int. 14 (1990) 20.
[27] K. Yoshida, I. Yamazaki, Y. Tozaki, N. Aoki, J.I. Yoshiyama, K. Arai, Tetsu-to-Hagane 76 (1990) 1817–1822.
[28] K. Shiwaku, S. Kawasaki, A. Kamimori, M. Aoki, K. Hajika, Tetsu-to-Hagane 73 (1987) 1567–1574.
[29] K. Kato, Y. Akabayashi, M. Kojima, Y. Nakamura, K. Kojima, S. Onoyama, CAMP-ISIJ 4 (1991) 1153.
[30] K. Kato, H. Yamauchi, S. Onoyama, M. Oita, T. Sado, M. Ina, CAMP-ISIJ 4 (1991) 1154.
[31] X.F. Jiang, Z.P. Chen, Z.X. Lu, G. Zhang, Z.M. Zhong, Rev. Métall. 104 (2007) 29–34.
[32] W. Wu, H.D. Meng, L. Liu, J. Iron Steel Res. Int. 20 (2013) No. 6, 7–12.
[33] X.H. Wang, J.Z. Li, F.G. Liu, Steelmaking 33 (2017) No. 1, 1–11, 55.
[34] T. Matsuo, I. Yamazaki, S. Masuda, K. Yoshida, A. Mori, S. Pukagawa, in: T. Matsuo, S. Fukagawa, T. Ikeda, S. Masuda, G.P. Schneider (Eds.), Proceedings of 73rd Steelmaking Conference, ISS, Warrendale, PA, USA, 1990, pp. 115–121.
[35] X.W. Su, H. Cui, B.L. Zhang, Y.Q. Liu, L. Luo, C.X. Ji, Journal of Chongqing University 41 (2018) 56–65.
[36] M.F. Xu, Y.T. Gao, A.B. Jin, Y. Zhou, L.J. Guo, G.S. Liu, Chinese Journal of Engineering 38 (2016) 1059–1068.
[37] N. Sasaki, K. Naito, Y. Demoto, S. Kitamura, Tetsu-to-Hagane 88 (2002) 300–305.
[38] X. Yang, H. Matsuura, F. Tsukihashi, ISIJ Int. 49 (2009) 1298–1307.
[39] H. Matsuura, T. Hamano, M. Zhong, X. Gao, X. Yang, F. Tsukihashi, JOM 66 (2014) 1572–1580.
[40] Y.C. Lü, X.H. Wang, D.P. Qin, Y. Liu, H.B. Wang, Iron and Steel 53 (2018) No. 6, 31–38.
[41] H. Suito, R. Inoue, ISIJ Int. 35 (1995) 258–265.
[42] Y. Ogasawara, Y. Miki, Y. Uchida, N. Kikuchi, ISIJ Int. 53 (2013) 1786–1793.
[43] H. Suito, R. Inoue, Trans. ISIJ 70 (1984) 186–193.
[44] H.G. Hadrys, M.G. Frohberg, Metall. Trans. 1 (1970) 1867.
[45] C.L. Zhao, Optimizing study of De-P steelmaking process in Shougang Jingtang, University of Science and Technology Beijing, Beijing, China, 2016.
[46] C.W. Bale, E. Belisle, P. Chartrand, S.A. Decterov, G. Eriksson, K. Hack, I.H. Jung, Y.B. Kang, J. Melancon, A.D. Pelton, C. Robelin, S. Petersen, Calphad 33 (2009) 295–311.
[47] Z.C. Zhao, Y.H. Sun, L. Luo, Z.L. Zhao, Steelmaking 31 (2015) No. 6, 13–16, 22.